Capturing Process of Debris Flow with Driftwood by an Open Type Check Dam

Badri Bhakta SHRESTHA*, Hajime NAKAGAWA, Kenji KAWAIKE, Yasuyuki BABA and Hao ZHANG

*Graduate School of Engineering, Kyoto University

Synopsis

A two-dimensional numerical model is developed for computing the characteristics of debris flow with driftwood and its capturing process by open type check dams such as grid or slit type check dam. A numerical model is developed with an interacting combination of Eulerian expression of the debris flow and Lagrangian expression of the driftwood, in which the fluctuation components of the position and the rotational angular velocity of the driftwood are dealt with stochastically. The jamming of driftwood on grid or slit type check dam is evaluated based on the geometric conditions and probabilistic approaches. The simulated results of outflow discharge, sediment discharge and the percentage of driftwood outflow at the downstream end of the flume agree well with the experimental results.

Keywords: debris flow, driftwood, open type check dam, capturing process, simulation

1. Introduction

Debris flow is a phenomenon that high-density water with mud and big gravel flows down along a stream at high speed, which occurs in a wide variety of environments throughout the world. Because of its high density and speed, it has huge destruction power. Thus damages by debris flows are very severe and sometimes tragic (Takahashi et al., 1992; Hunt, 1994; Huang and Garcia, 1997; Nakagawa et al., 2000; Shrestha et al., 2008). In recent years much driftwood has combined with debris flow. Such driftwood clogs narrows in the river course or bridge or culvert sites giving rise to flooding, bridge/piers or embankments damage or destruction (Shrestha et al., 2009). Fig. 1 shows the observed yield quantities of driftwood carried by debris flow in both coniferous and broadleaf forests of Japan. Thus, the studies on behavior of debris flow with driftwood and structural and non-structural countermeasures against debris flow disasters with driftwood are very important in order to reduce the extensive property damage and loss of life due to debris flow disasters with driftwood. It is also necessary to understand the mechanism of debris flow with driftwood behavior to clarify the nature of debris flow disasters with driftwood.

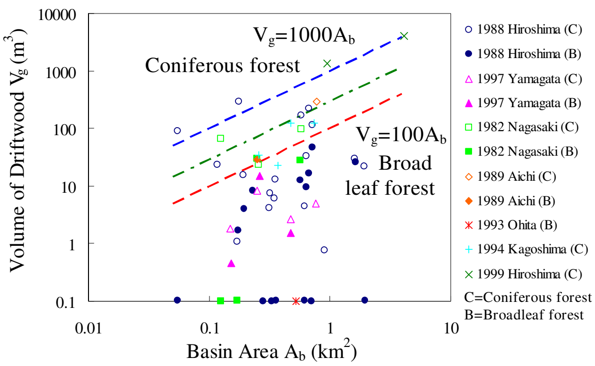

Fig. 1 Basin area and volume of driftwood carried by debris flow in both coniferous and broadleaf forests of Japan *(Source: Sabo Department, Ministry of Construction, Japan, 2000)*

Fig. 2 Debris flow and driftwood captured by grid dam at Agi River, Nakatsugawa, Gifu Pref., Japan, 2000 (*Source: Sabo Department, MLIT, Japan)*

Fig. 3 Debris flow and driftwood captured by sabo dam at Tenryu River, Okaya, Nagano Pref., Japan, 2006 (*Source: Sabo Department, MLIT, Japan)*

Many researchers such as Takahashi et al. (1992), Egashira (1993), Nakagawa et al. (1996), Honda and Egashira (1997), Inverson (2003) and others have proposed numerical models of debris flow as a mixture of sediment and water, but they have not considered the behavior of debris flow with driftwood. On the other hand, some numerical studies to compute the behavior of driftwood only with clear water flow have been carried out by Nakagawa et al. (1994, 1995), Gotoh et al. (2002), Shimizu and Osada (2008) and few others, but they have not focused on computing the behavior of driftwood with debris flow or sediment water mixture flow.

Open type check dams such as grid type or slit type check dams are commonly used for debris flow control and capturing driftwood because they are preferable over closed type check dams for conserving the natural environment and landscape of mountain torrents as much as possible. In the debris flow section where driftwood is assumed to flow down with a debris flow, both of them are captured together by the open type check dam. Fig. 2 and Fig. 3 show the examples of debris flow and driftwood captured by grid dam at Agi River, Gifu Prefecture, Japan and by sabo dam at Tenryu River, Nagano Prefecture, Japan, respectively. Many researchers have investigated debris flow capturing by check dams considering sediments of the flow only (Takahashi et al., 2001; Satofuka and Mizuyama, 2006; Shrestha et al., 2008). Only few research works have been carried out on capturing of debris flow and driftwood by check dams (Ozaki et al., 1998; Doi et al., 2000; Katatani and Yamada, 2006). Furthermore, these studies are limited to the experimental study only.

In this study, a two-dimensional numerical model is developed for computing the behavior of debris flow with driftwood and its capturing process due to jamming of driftwood on open type check dams such as grid or slit dam. A numerical model has been developed with an interacting combination of Eulerian expression of the debris flow and Lagrangian expression of the driftwood, in which the fluctuation components of the position and the rotational angular velocity of the driftwood are dealt with stochastically as random variables based on the results of a statistical analysis of experimental values. The motion of driftwood is restricted near the flow surface. The simulated results of outflow discharge and the percentage of driftwood outflow at the downstream end of the flume are compared with those obtained from hydraulic model experiments.

2. Numerical model

2.1 Basic equations of debris flow motion

The basic equations used to compute the behavior of flow motion of debris flow are the two-dimensional momentum equations, continuity equation of flow, continuity equation of sediment and river bed surface equation. The motion of driftwood is restricted near the flow surface and the shear stresses at the flow surface are generated as the reaction of the drag force acting on the driftwood. By introducing these shear stresses at the flow surface, the depth-wise averaged two-dimensional momentum equations of debris flow for the x–wise (down valley) and y-wise (lateral) directions are described as follows.

$$\frac{\partial M}{\partial t}+\beta\frac{\partial(uM)}{\partial x}+\beta\frac{\partial(vM)}{\partial y}=gh\sin\theta_{bx0} -gh\cos\theta_{bx0}\frac{\partial(z_b+h)}{\partial x}-\frac{\tau_{bx}}{\rho_T}+\frac{\tau_{sx}}{\rho_T} \quad (1)$$

$$\frac{\partial N}{\partial t}+\beta\frac{\partial(uN)}{\partial x}+\beta\frac{\partial(vN)}{\partial y}=gh\sin\theta_{by0} -gh\cos\theta_{by0}\frac{\partial(z_b+h)}{\partial y}-\frac{\tau_{by}}{\rho_T}+\frac{\tau_{sy}}{\rho_T} \quad (2)$$

The continuity equation of the total volume is

$$\frac{\partial h}{\partial t}+\frac{\partial M}{\partial x}+\frac{\partial N}{\partial y}=i_b \quad (3)$$

The continuity equation of the sediment particle fraction is

$$\frac{\partial(Ch)}{\partial t}+\frac{\partial(CM)}{\partial x}+\frac{\partial(CN)}{\partial y}=i_bC_* \quad (4)$$

The equation for the change of bed surface elevation is

$$\frac{\partial z_b}{\partial t}+i_b=0 \quad (5)$$

where M $(=uh)$ and N $(=vh)$ are the flow discharge per unit width in x and y directions, u and v are the velocity components in x and y directions, h is the flow depth, z_b is erosion or deposition thickness of the bed measured from the original bed surface elevation, θ_{bx0} and θ_{by0} are the x and y components of slope of the original bed surface, i_b is erosion/deposition velocity used as Takahashi et al. (1992), C is the sediment concentration in the flow, C_* is the sediment concentration in the bed, β is the momentum correction factor equal to 1.25 for a stony debris flow (Takahashi et al., 1992) and to 1.0 for both an immature debris flow and a turbulent flow, g is the acceleration due to gravity, τ_{bx} and τ_{by} are the bottom shear stresses in x and y directions used as Takahashi (2007), ρ_T is mixture density ($\rho_T=\sigma C+(1-C)\rho$, σ is density of the sediment particle and ρ is density of the water), and τ_{sx} and τ_{sy} are the shear stresses at the flow surface in x and y directions generated as the reaction of the drag force acting on the driftwood as follows:

$$\tau_{sx}=\frac{1}{A}\sum_{k=1}^{N_t}\left\{\frac{1}{2}\rho_T C_{Dx}W_k(u_k-U_k)A_{kx}\right\} \quad (6)$$

$$\tau_{sy}=\frac{1}{A}\sum_{k=1}^{N_t}\left\{\frac{1}{2}\rho_T C_{Dy}W_k(v_k-V_k)A_{ky}\right\} \quad (7)$$

where u_k and v_k are the respective driftwood velocity components in x and y directions, U_k and V_k are the respective local velocity components of the fluid in x and y directions at the position of the centroid of the driftwood, $W_k=\sqrt{(u_k-U_k)^2+(v_k-V_k)^2}$, A_{kx} and A_{ky} are the respective projected areas of the submerged part of the driftwood in x and y directions, C_{Dx} and C_{Dy} are the drag coefficients in x and y directions, A $(=\Delta x\Delta y)$ is the area of the flow surface (Δx and Δy are the grid sizes of the finite difference equations), and N_t is the number of total pieces of driftwood in area A.

As the motion of the piece of driftwood is restricted near the flow surface, the surface flow velocity components are calculated as Takahashi (1991).

2.2 Basic equations of driftwood motion

It is assumed that the pieces of driftwood are sufficiently dispersed so that collisions between them are infrequent. The equations of motion of each piece of driftwood, individually labeled by subscript k are expressed as

$$\frac{dX_k}{dt}=u_k \quad ; \quad \frac{dY_k}{dt}=v_k \quad (8)$$

$$(m_k+mC_M)\frac{du_k}{dt}=-m_kg\frac{\partial H_k}{\partial x} -\frac{1}{2}\rho_T C_{Dx}W_k(u_k-U_k)A_{kx} \quad (9)$$

$$(m_k+mC_M)\frac{dv_k}{dt}=-m_kg\frac{\partial H_k}{\partial y} -\frac{1}{2}\rho_T C_{Dy}W_k(v_k-V_k)A_{ky} \quad (10)$$

where X_k and Y_k are the position of the centroid of the driftwood, m_k is the mass of the driftwood, m is the mass of the fluid occupied by volume of a piece of driftwood, C_M is the virtual mass coefficient, and H_k is the flow level at centroid position of the driftwood.

The rotational motion around the axis of the centroid of the driftwood is described by evaluating the moment N_0 produced by the hydrodynamic force acting on the driftwood as

$$Id^2\theta_k / dt^2 = \sum N_0 \tag{11}$$

where θ_k is the rotational angle of the piece of driftwood and I is the moment of inertia around the centroid. The rotational motion of driftwood is also supposed to be restricted on the flow surface and the rotation on the vertical plane is not considered.

2.3 Fluctuation of position and rotational angle of driftwood

(1) Fluctuation of position of driftwood

Driftwood positions can be evaluated by integrating Equation (8) deterministically under suitable initial conditions, but they fluctuate due to the collision of driftwood with boulders and disturbances on the flow surface during the collision of the sediment particles, which are considered in the diffusions coefficients. The diffusion coefficients are determined from the hydraulic model experiments with interacting driftwood and sediment-water mixture flow. The fluctuation components of driftwood position ΔX_k and ΔY_k are evaluated as Nakagawa et al. (1994, 1995).

$$\Delta X_k = \sqrt{4K_x(2\Delta t)}erf^{-1}(\alpha') \tag{12}$$

$$\Delta Y_k = \sqrt{4K_y(2\Delta t)}erf^{-1}(\beta') \tag{13}$$

where K_x and K_y are the longitudinal and transverse diffusion coefficients, α' and β' are random variables uniformly distributed in the range (0,1), and erf^{-1} is the inverse of error function, erf, given by

$$\left.\begin{aligned} erf(s) &= \left\{1 - \Phi(\sqrt{2}s)\right\} = \left(1/\sqrt{\pi}\right)\int_s^{\infty} \exp(-\varepsilon^2)d\varepsilon \\ \Phi(s) &= \left(1/\sqrt{2\pi}\right)\int_{-\infty}^{s} \exp(-\varepsilon^2/2)d\varepsilon \end{aligned}\right\} \tag{14}$$

The driftwood position is estimated by adding the fluctuation value to the value obtained from the equations of motion deterministically as

$$X_k^{n+3} = X_k^{n+1} + u_k^{n+2}(2\Delta t) + \sqrt{4K_x(2\Delta t)}erf^{-1}(\alpha') \tag{15}$$

$$Y_k^{n+3} = Y_k^{n+1} + v_k^{n+2}(2\Delta t) + \sqrt{4K_y(2\Delta t)}erf^{-1}(\beta') \tag{16}$$

(2) Fluctuation of rotational angle of driftwood

The rotational angle of a piece of driftwood can be evaluated deterministically by solving Equation (11), but it also fluctuates due to the collision of driftwood with boulders and disturbances on the flow surface during the collision of the sediment particles. Therefore, the rotational angle of driftwood is evaluated by considering the fluctuation component as follows.

$$d\theta_k / dt = \omega_d + \omega_p \tag{17}$$

$$\theta_k^{n+3} = \theta_k^{n+1} + 2\Delta t(\omega_d + \omega_p) \tag{18}$$

where ω_d is the angular velocity of the piece of driftwood obtained deterministically and ω_p is the fluctuation of the angular velocity of the driftwood evaluated stochastically. Assuming the rotational angular velocity of the fluctuating component of a piece of driftwood follows a normal distribution, its distribution function, Φ, is given by

$$\Phi(\gamma) = \frac{1}{\sqrt{2\pi}}\int_{-\infty}^{\gamma} \exp(-\varepsilon^2/2)d\varepsilon \tag{19}$$

where $\gamma = (\omega_p - \overline{\omega})/\sigma_w$ is obtained from the inverse function, Φ^{-1}, for uniformly distributed

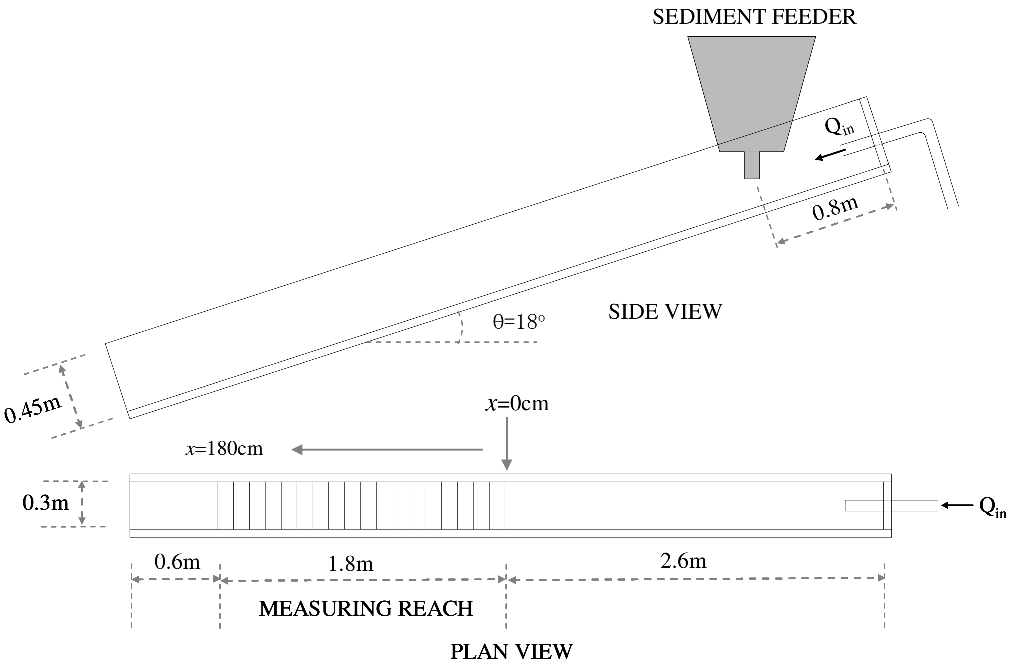

Fig. 4 Experimental setup for determination of diffusion coefficients and rotational angular velocity of driftwood

Table 1 Experimental conditions and results of diffusion coefficient and rotational angle of driftwood

EXP NO.	Q_{in} (cm^3/sec)	Q_{flow} (cm^3/sec)	C	h (cm)	u (cm/sec)	u_* (cm/sec)	Fr	$\frac{K_x}{u_* h}$	$\frac{K_y}{u_* h}$	$\overline{\varpi}$ (deg/sec)	σ_w (deg/sec)
1	646.020	843.489	0.283	0.830	33.875	15.854	1.188	0.856	0.487	-0.881	28.896
2	742.105	976.006	0.320	0.900	36.148	16.509	1.217	0.930	0.323	0.550	29.645
3	888.563	1028.305	0.323	0.910	37.667	16.601	1.261	0.278	0.389	0.727	38.970
4	993.644	1538.425	0.340	1.100	46.619	18.252	1.420	0.709	0.293	-2.385	41.134
5	873.729	1130.734	0.265	0.960	39.262	17.051	1.280	0.543	0.408	-2.099	27.268
6	924.146	1215.897	0.270	0.990	40.939	17.315	1.314	0.829	0.271	0.470	34.483
7	844.030	1318.343	0.339	1.030	42.665	17.661	1.343	0.774	0.244	1.518	33.945
8	873.627	1284.487	0.269	1.020	41.977	17.575	1.328	0.272	0.330	-2.611	30.291
Mean								**0.649**	**0.343**	**-0.589**	**33.079**

random numbers within (0,1), $\overline{\varpi}$ and σ_w are the mean and standard deviation of angular velocity of driftwood. After γ is obtained, ω_p is estimated from $\omega_p = \gamma\sigma_w + \overline{\varpi}$.

3. Determination of diffusion coefficients and rotational angle of driftwood

3.1 Laboratory experiments and method

A rectangular flume of 5m long, 30cm wide and 45cm deep is used for the experiments. The slope of the flume is set at 18 degrees. To measure the position and rotational angle of the driftwood, 19 pieces measuring rods having the same length as the flume width, are stretched across the flume at intervals of 10cm in the downstream direction from x = 0 cm (2.6m downstream from the upstream end) along the 1.8m measuring reach (Fig. 4). Sediment (mean size = 1.86mm, maximum size = 4.75mm) is supplied with a sediment feeder at 0.8m

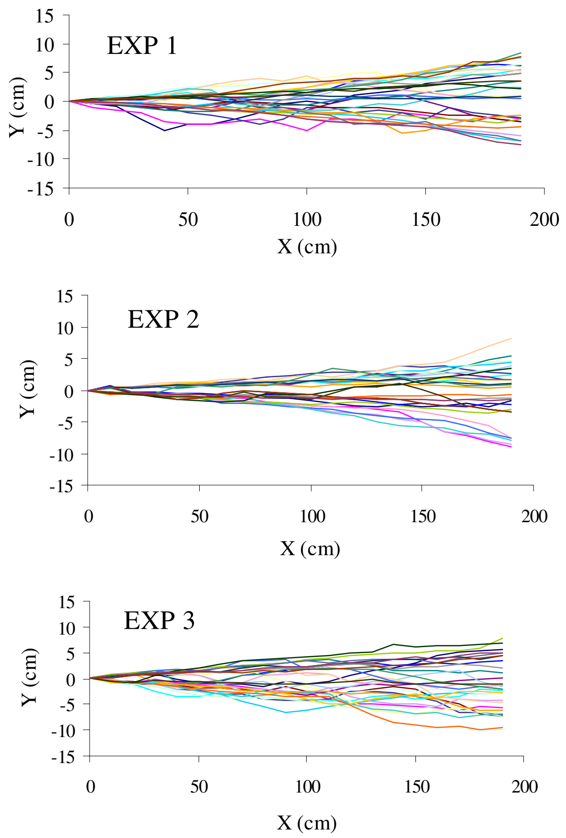

Fig. 5 Path lines of the centroid of the driftwood

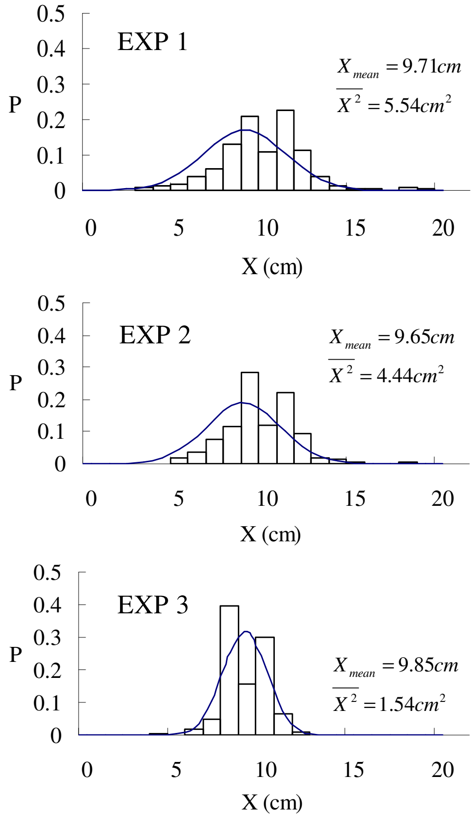

Fig. 6 Frequency distribution of longitudinal position of driftwood

downstream from the upstream end and water discharge is supplied from the upstream end of the flume. A piece of driftwood is supplied at x= -10cm after supplying designated water and sediment mixture flow discharge. The position and rotational angle of the moving driftwood are measured with a video camera in each of the 19 sections for x = 0, 10, 20,…..180cm. Such measurement is repeated 30 times for each experiment under the same hydraulic conditions.

A 3.5cm long, cylindrical piece of driftwood with a diameter of 3mm and a mass density $\rho_d = 0.785$g/cm^3 is used. The data obtained in the experiments are analyzed statistically, after which the diffusion coefficients and other hydraulic parameters are determined.

The experimental conditions and results are shown in Table 1, where Q_{in} is the upstream end inflow water discharge, Q_{flow} is sediment-water mixture flow discharge in the flume, C is the sediment concentration in the flow, h is the flow depth, u is the cross-sectional averaged velocity of the flow, $u_* = \sqrt{gh\sin\theta}$ is the friction velocity (θ= flume slope) and $Fr = u/\sqrt{gh}$ is the Froude number. Eight experiments are carried out with different hydraulic conditions.

3.2 Diffusion coefficients of driftwood

Fig. 5 shows the path lines of centroids of the driftwood of 30 pieces of driftwood and it demonstrates statistical variety of them. The scattering process of driftwood is described as a diffusion process and the diffusion coefficients might be defined. The frequency distributions of longitudinal and transverse positions of driftwood are shown in Fig. 6 and Fig. 7 respectively, in which solid line is calculated from the normal distribution. The longitudinal and transverse diffusion coefficients of the driftwood are evaluated as follows:

$$K_x = (1/2)(\overline{dX^2}/dt) \tag{20}$$

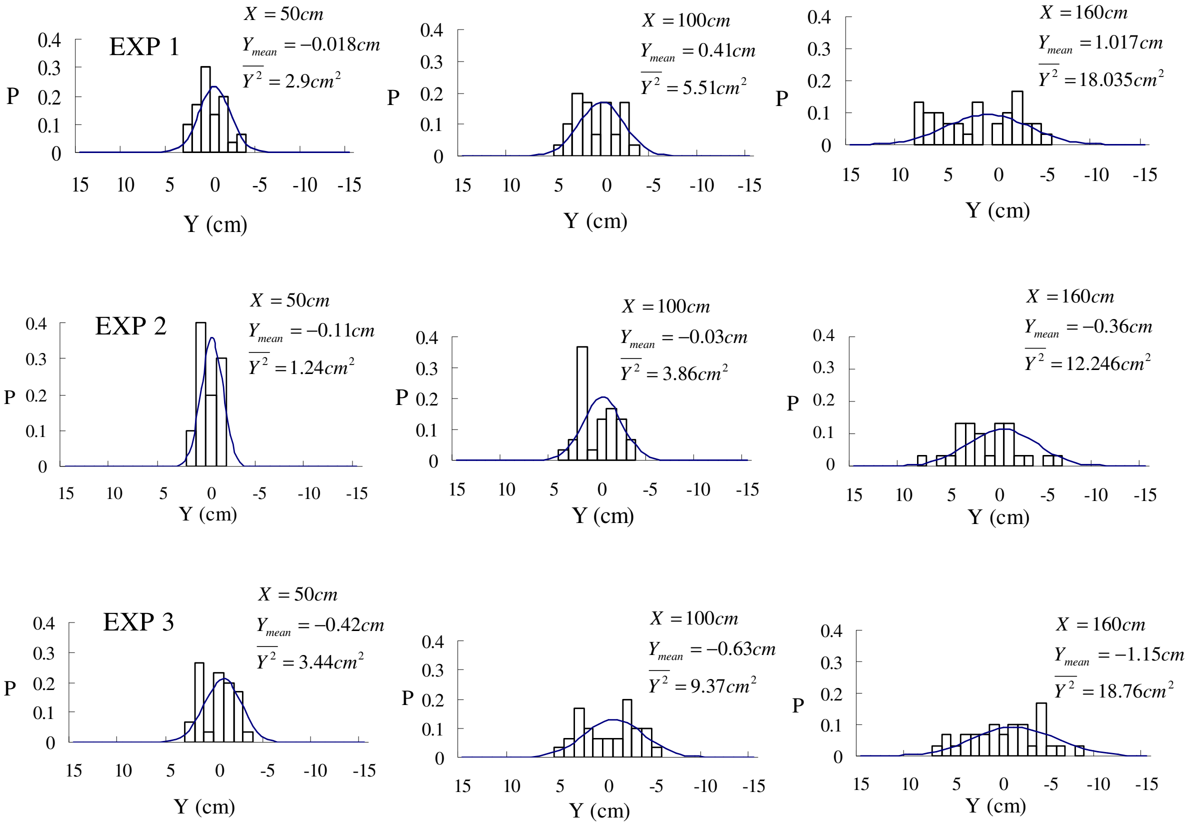

Fig. 7 Frequency distribution of transverse position of driftwood

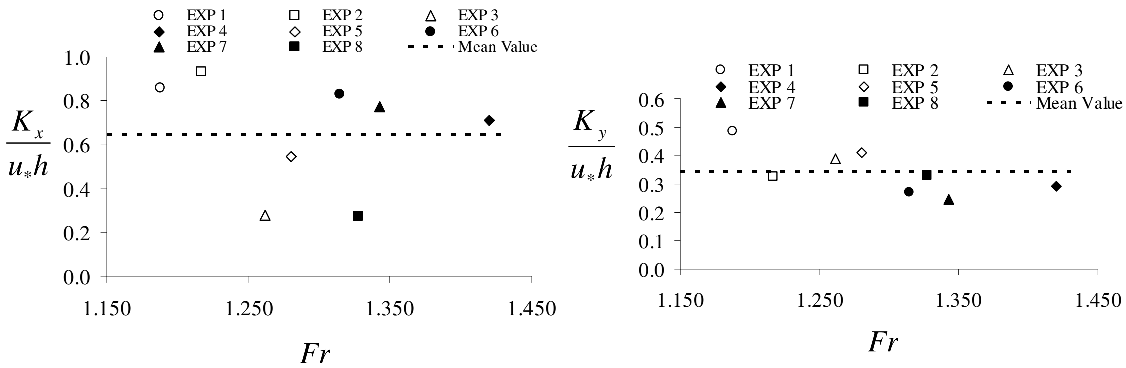

Fig. 8 Relation of non-dimensional diffusion coefficients and Froude number

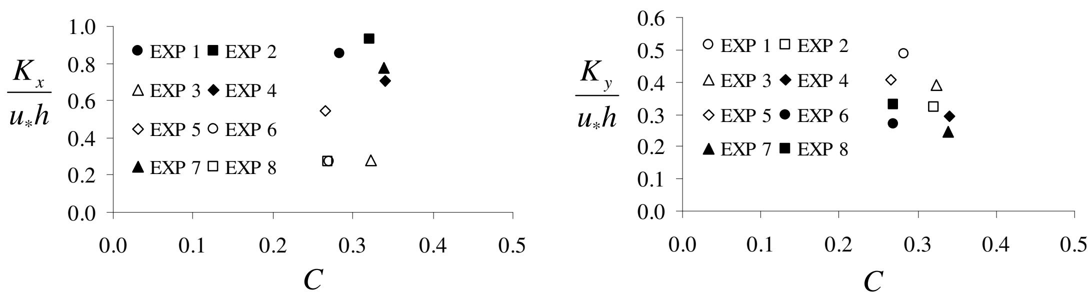

Fig. 9 Relation of non-dimensional diffusion coefficients and sediment concentration

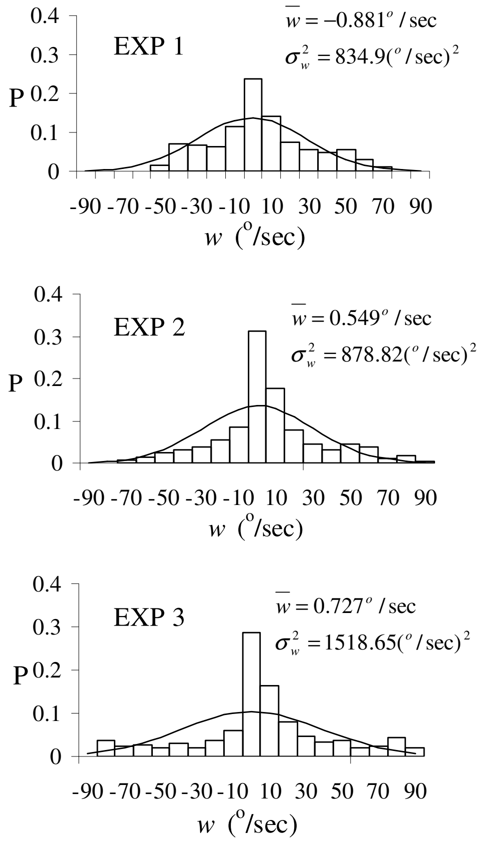

Fig. 10 Frequency distribution of the rotational angular velocities of the driftwood

$$K_y = (1/2)(\overline{dY^2}/dt) \tag{21}$$

where $\overline{X^2}$ and $\overline{Y^2}$ are the longitudinal and transverse variances. Table 1 shows the calculated results of diffusion coefficients. The average values of non-dimensional diffusion coefficients $K_x/u_*h = 0.649$ and $K_y/u_*h = 0.343$ are obtained. The relations of non-dimensional diffusion coefficients with Froude number and sediment concentration are shown in Fig. 8 and Fig. 9, respectively.

3.3 Rotational angle of driftwood

Frequency distribution of the rotational angular velocities of driftwood obtained experimentally is shown in Fig. 10, in which solid line is calculated by assuming the normal distribution with values of the parameters determined from the experiments. The mean value of the angular velocities is approximately zero, $\overline{\omega} \approx 0$. The standard deviation

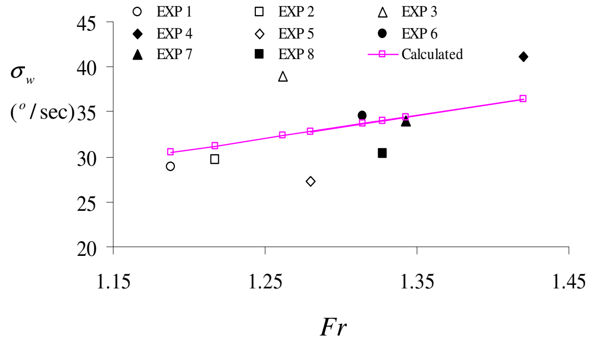

Fig. 11 Relation of Froude number, Fr, to standard deviation, σ_w, of the rotational angular velocities of the driftwood

appears to be prescribed by the hydraulic parameters, and it is related to the Froude number. The relation between the Froude number, Fr, and the standard deviation of the rotational angular velocity of the driftwood, σ_w, is shown in Fig. 11, and the relation is obtained as $\sigma_w = 25.61Fr$.

4. Experiments of debris flow with driftwood

To investigate the capturing process of debris flow with driftwood by open type check dams and the verification of the model, a series of experiments are carried out. For the experiments, a rectangular flume of 5m long, 10cm wide and 13cm deep is used. The experiments are carried out for flume slope of 18 degrees. Fig. 12 shows the detail of experimental setup. Check dams are set at 20cm upstream from the downstream end of the flume. Fig. 13 shows the details of check dams. A sediment bed of 1.9m long and 7cm deep is positioned from 2.8m to 4.7m upstream measured from the outlet of the flume. Sediment materials with mean diameter d_m = 2.39mm, maximum diameter $d_{\max} = 11.2$mm, $\tan\phi = 0.7$ (ϕ =angle of repose) and sediment density σ = 2.65g/cm^3 are used. The sediment materials are prepared by mixing the uniformly distributed different sizes of silica sands and gravels. The particle size distribution of sediment mixture is shown in Fig. 14. Cylindrical pieces of 38 driftwood pieces (Ramin wood, ρ_d = 0.785g/cm^3) are positioned on the sediment bed at intervals of 10cm c/c along the

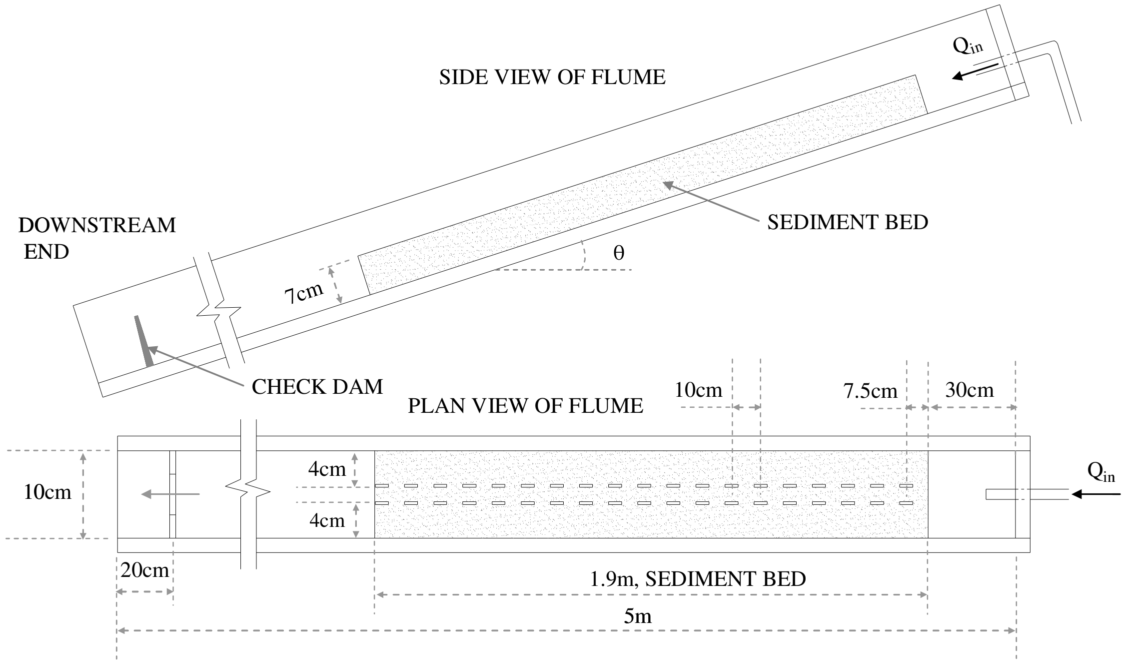

Fig. 12 Experimental setup and positions of the driftwood for the experiments

downstream direction from 7.5cm downstream from the upstream end of the sediment bed in two columns 2cm apart as shown in Fig. 12. The sediment bed is saturated by water. Debris flow is produced by supplying a constant water discharge 270cm^3/sec for 10sec from the upstream end of the flume. The experiments are carried out for driftwood pieces of diameter 3mm and 4mm with 3.5cm, 4.0cm and 4.5cm in length.

The experiments are repeated three times under the same identical conditions, because the sediment composition and degree of saturation might not be uniform throughout the sediment layer. The flow discharge and driftwood at downstream end of the flume are determined by collecting outflow discharge using series of manually movable sampler boxes. The jamming of driftwood and deposition upstream of check dams are evaluated by capturing the images shot by video cameras located at side, front and above the downstream end of the flume. The flow motion of driftwood at forefront of debris flow in the experiment is shown in Fig. 15. Fig. 16 shows the flow motion of driftwood at upstream of grid and slit type check dams and sediment deposition behind check dams due to driftwood jamming. Fig. 17 shows the final depth of debris

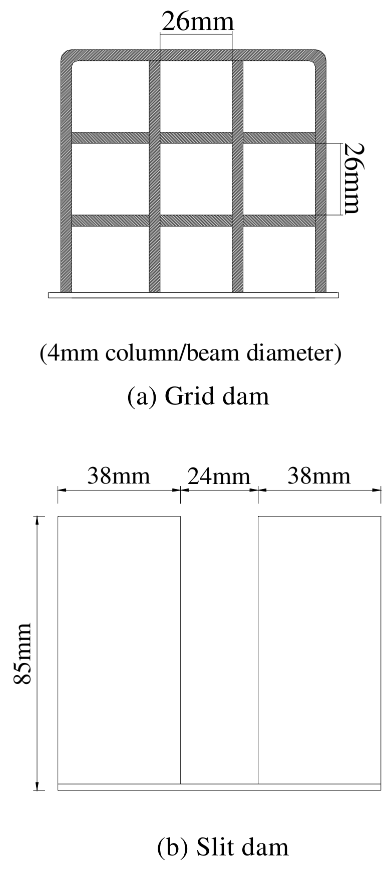

Fig. 13 Details of check dams (a) Grid dam, (b) Slit dam

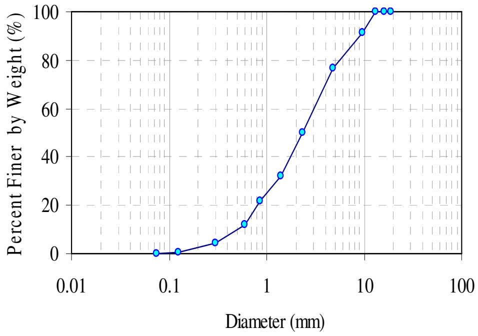

Fig. 14 Particle size distribution curve of bed sediment

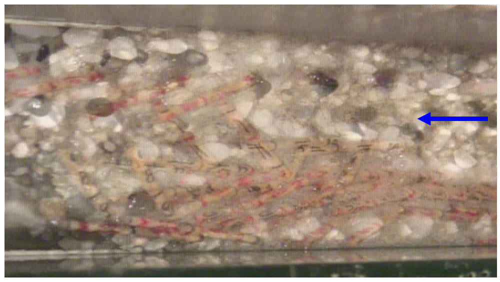

Fig. 15 Flow motion of driftwood at forefront of debris flow

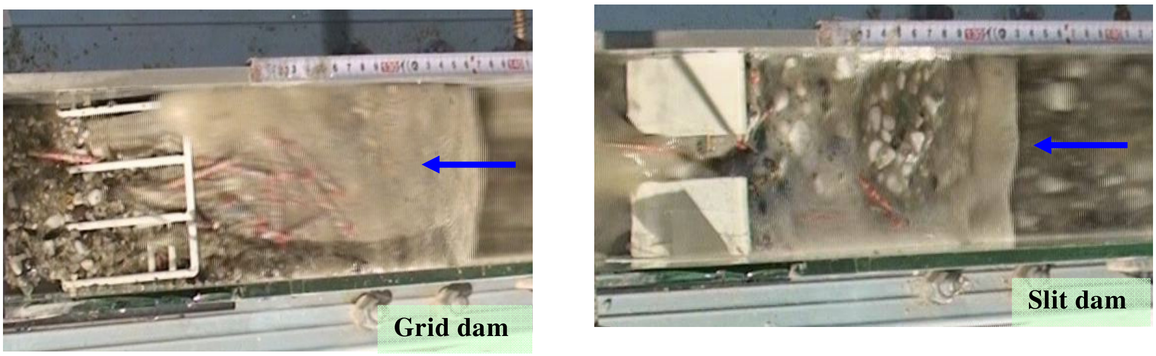

Fig. 16 Flow motion of driftwood at upstream of check dams

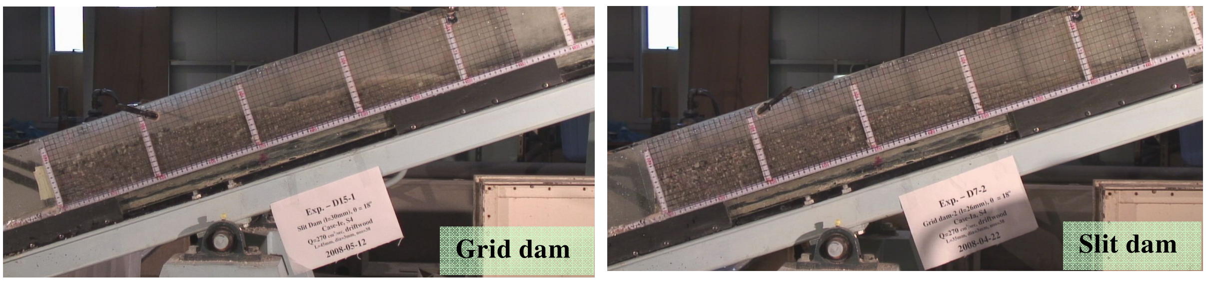

Fig. 17 Final depth of sediment deposition upstream of grid and slit type check dams

flow deposition upstream of grid and slit type check dams in the experiments.

5. Driftwood Jamming and debris flow deposition

5.1 Driftwood jamming

When the driftwood is jammed on open space of open type check dam such as grid or slit dam, the sediment is deposited upstream side of the dam. The jamming of driftwood on open type check dams is evaluated based on the geometric conditions and probabilistic approaches as follows.

(1) Driftwood jamming on grid dam

Four cases are considered as conditions under which driftwood is jammed on open spaces of a grid dam: (1) a piece of driftwood with a large rotational angle (Fig. 18 (a)). On the basis of the experimental results, it is considered that the rotational angle of

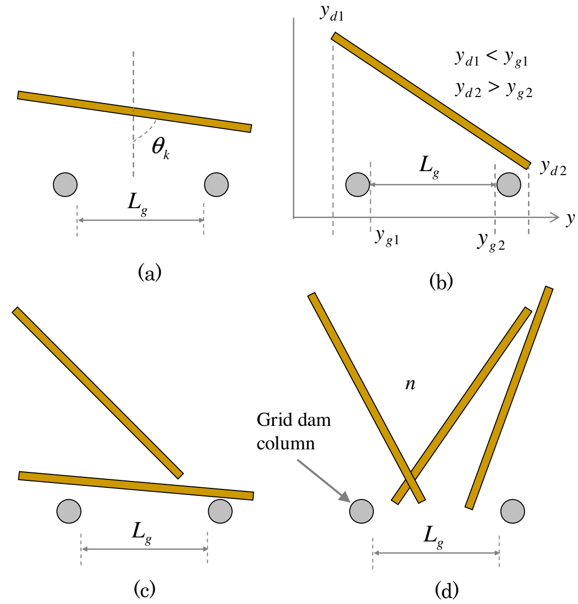

Fig. 18 Jamming of driftwood on grid dam

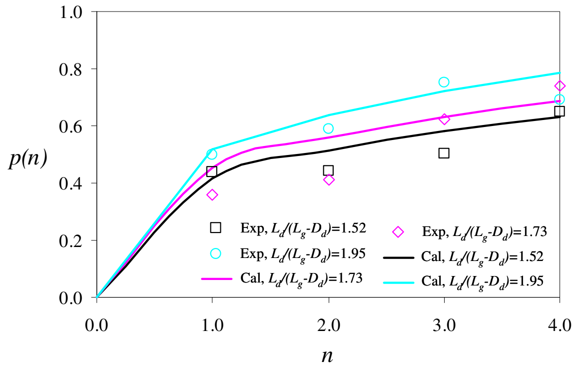

Fig. 19 Plot of jamming probability, $p(n)$, and number of driftwood arrival, n, using Equation (22) with experimental data for grid dam

the driftwood to be in the range of $80^o \le \theta_k \le 90^o$. (2) A piece of driftwood will be jammed on a grid dam due to geometric conditions as $y_{d1} < y_{g1}$ and $y_{d2} > y_{g2}$ (Fig. 18 (b)). (3) A piece of driftwood coming from the rear will be also jammed by the pieces of driftwood already jammed on a grid dam (Fig. 18 (c)). It is considered that when more than five pieces of driftwood already jammed at previous time level of calculation, all pieces of driftwood coming from the rear are also considered to be jammed on a grid dam. (4) The pieces of driftwood will be jammed when the number of pieces of driftwood arrival at grid opening at same time (Fig. 18 (d)). In this case, the probability of a piece of driftwood jamming depends on the number of driftwood arrival at grid opening at same time. This probability, $p(n)$, can be assessed in hydraulic experiments with assuming the functions of length (L_d) and diameter (D_d) of driftwood, clear spacing between two columns of grid dam (L_g) and number of driftwood (n) arrival at same time. The following relation is obtained from the experimental values as

$$p(n) = 0.32\left(\frac{L_d}{L_g - D_d}\right)^{0.63} n^{0.3} \qquad (22)$$

This equation is represented in Fig. 19 with experimental values. To determine which pieces of driftwood will be jammed, the random variable, q, uniformly distributed in the range (0,1), is generated for each piece of driftwood flowing down the flume. The driftwood is considered to be jammed when the condition $p(n) > q$ is satisfied.

(2) Driftwood jamming on slit dam

Five cases are considered as conditions under which driftwood is jammed on a slit dam. The four conditions of driftwood jamming on slit dam are similar to as grid dam case (Fig. 20 (a), (b), (c) and (d)). In the case of slit dam, the relation of the probability of a pieces of driftwood jamming, $p(n)$, with the number of pieces of driftwood arrival at slit opening at a same time, n, is obtained as

$$p(n) = 0.23\left(\frac{L_d}{b - D_d}\right)^{1.02} n^{0.28} \qquad (23)$$

where b is width of slit opening. Equation (23) is represented in Fig. 21. Another additional condition for driftwood jamming on slit dam is described as follows. A piece of driftwood will be jammed in impermeable width (b_p) of slit dam when the centroid of the driftwood is located only inside dead zone of the flow as shown in Fig. 20 (e). When the centroid of the driftwood is located outside of dead zone, it can be carried by coming flow from

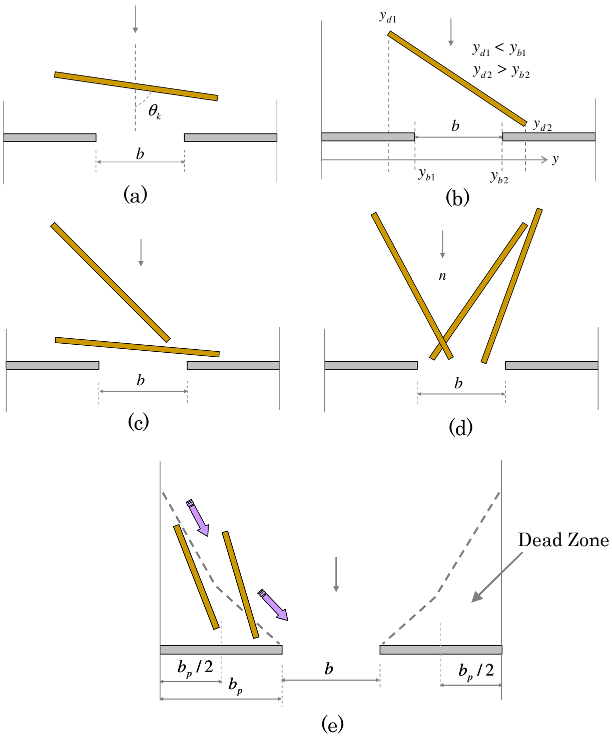

Fig. 20 Jamming of driftwood on slit dam

upstream. In this case, it is considered that when the centroid of a piece of driftwood is located inside half distance of impermeable width ($b_p/2$) from the channel wall, a piece of driftwood is considered to be jammed on slit dam.

5.2 Debris flow deposition

Due to the jamming of driftwood on a grid dam, sediment is deposited behind the grid dam. The effects of the driftwood jamming on debris flow deposition at grid dam is evaluated based on the projected horizontal length of driftwood piece in y direction with its rotational angle and clear spacing of column of grid dam, and the sediment passing rate, P_s, through a grid dam is determined as $P_s = L_o / L_g$ (Fig. 22). The deposition velocity, i_{dep}, is derived under the mass conservation law of sediment discharge per unit width (Q_{sed}) and sediment deposition as

$$\left.\begin{aligned} C_*\Delta x\Delta z &= (1-P_s)Q_{sed}\Delta t \\ i_{dep} &= -\Delta z/\Delta t = -(1-P_s)Q_{sed}/(C_*\Delta x) \end{aligned}\right\} \tag{24}$$

where Δx is the distance increment of calculating point and Δz is the thickness of the deposition.

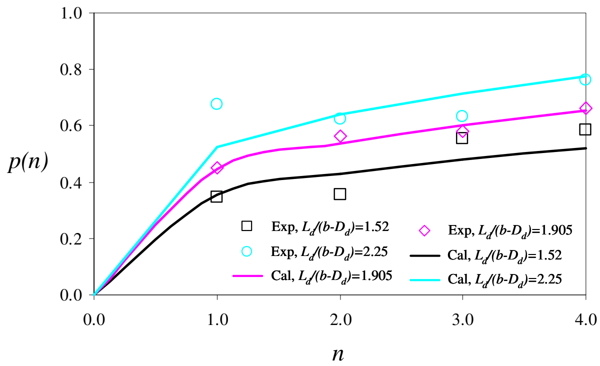

Fig. 21 Plot of jamming probability, $p(n)$, and number of driftwood arrival, n, using Equation (23) with experimental data for slit dam

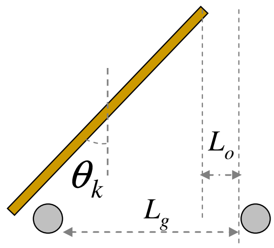

Fig. 22 Schematic diagram for sediment passing rate through grid dam

In the case of slit dam, the deposition equation due to jamming of driftwood on open space of slit dam similar to as grid dam is described as

$$i_{dep} = -(1-P_s)Q_{sed}/(C_*\Delta x) \tag{25}$$

in which $P_s = L_o / b$ is the sediment passing rate through open spacing of slit dam.

The open spaces of grid dam may be also blockaded by large boulders, and growing rate formula developed by Satofuka and Mizuyama (2006) is also considered. In the case of slit dam, the deposition velocity, i_{dep}, behind a slit dam caused by clogging of open space due to simultaneous arrival of two or more particles are described as follows:

$$i_{dep} = -K_{sd}(1-P_{sd})\frac{Q_{sed}}{C_*\Delta x} \tag{26}$$

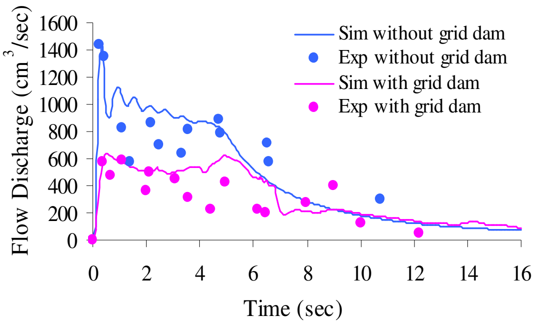

(a) Case with driftwood D_d=3mm and L_d =3.5cm

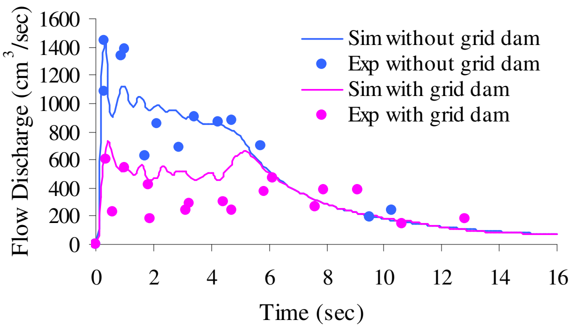

(b) Case with driftwood D_d=3mm and L_d =4.0cm

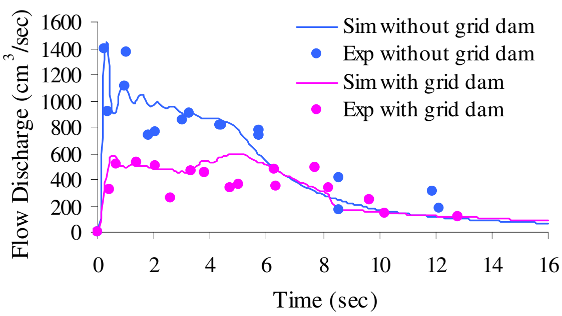

(c) Case with driftwood D_d=3mm and L_d =4.5cm

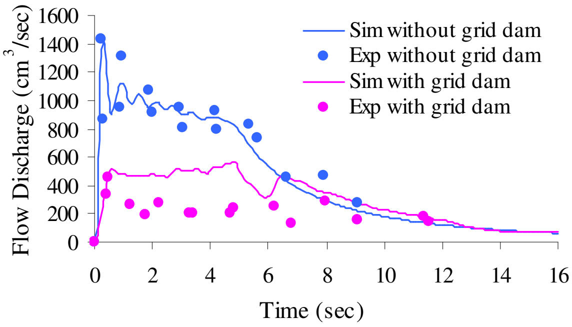

(d) Case with driftwood D_d=4mm and L_d =3.5cm

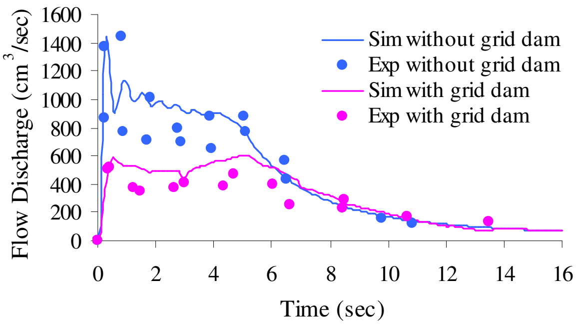

(e) Case with driftwood D_d=4mm and L_d =4.5cm

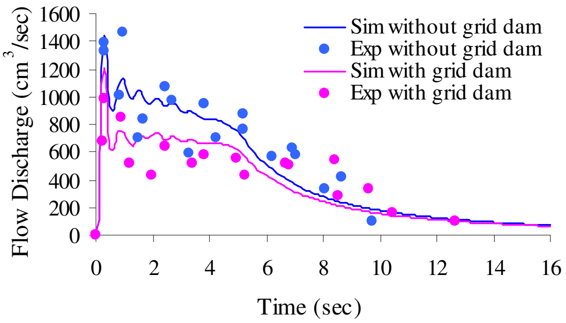

(f) Flow without driftwood case

Fig. 23 Flow discharge at downstream end of flume and discharge reduction by grid dam due to driftwood jamming

where $P_{sd} = (b-d)/b$ (d is diameter of particle) the sediment passing rate through slit dam, K_{sd} is numerical constant and Q_{sed} is sediment discharge per unit width.

The deposition velocity equation upstream of a check dam developed by Shrestha et al. (2008) is also employed to calculate debris flow deposition in the upstream area of check dam.

6. Results and discussions

The numerical simulations and experiments are performed to investigate the capturing process of debris flow with driftwood by open type check dams such as grid or slit type check dams. The jamming of driftwood on grid or slit dam is evaluated based on the geometric conditions and the probabilistic approaches. The geometric conditions under which jamming of driftwood on grid or slit dam are determined based on the evaluation of the experimental results, and probabilistic approach is developed from the regression analysis of the values obtained in the experiments. Debris flow deposition behind a grid or slit dam due to

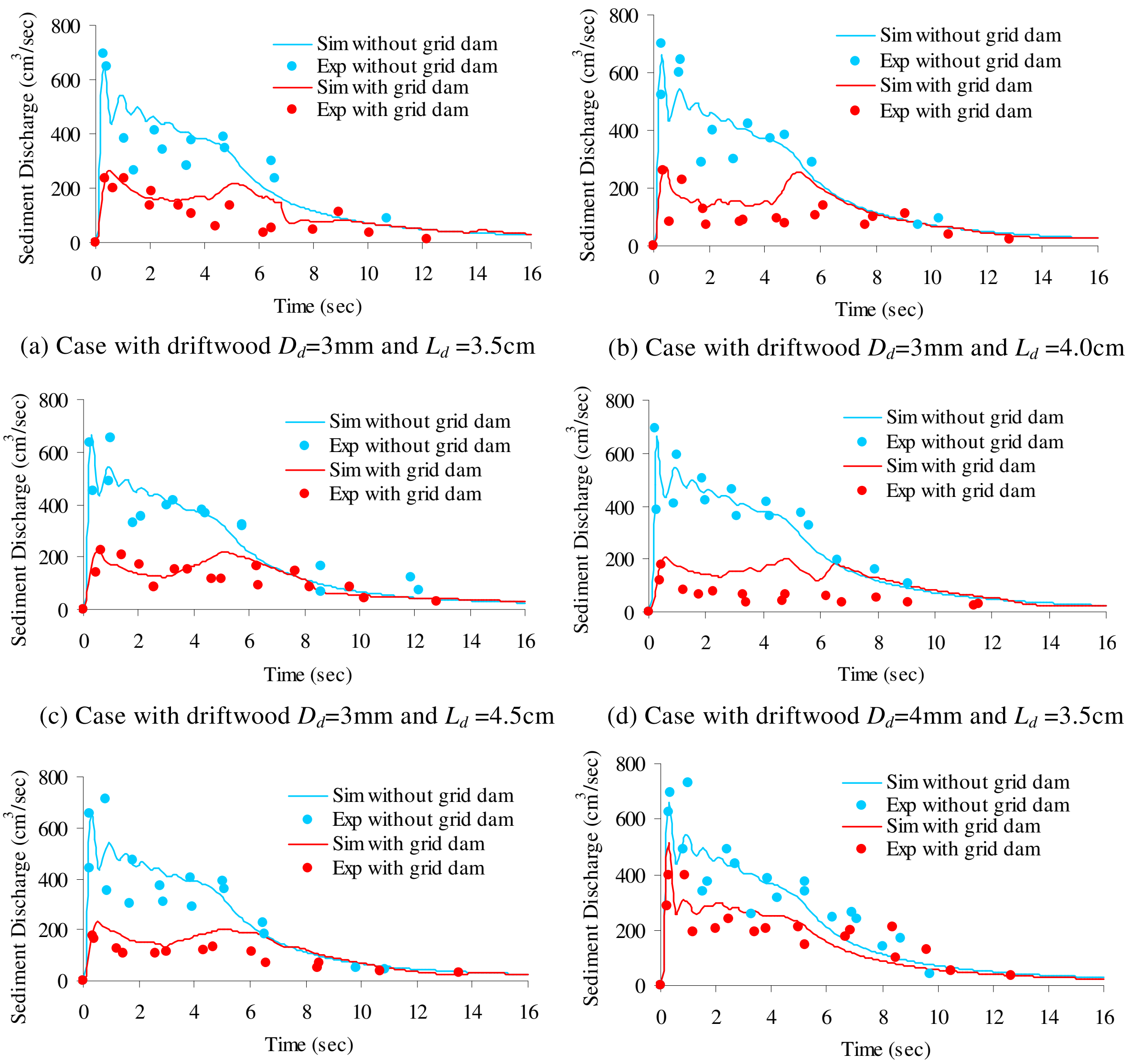

(a) Case with driftwood D_d=3mm and L_d =3.5cm

(b) Case with driftwood D_d=3mm and L_d =4.0cm

(c) Case with driftwood D_d=3mm and L_d =4.5cm

(d) Case with driftwood D_d=4mm and L_d =3.5cm

(e) Case with driftwood D_d=4mm and L_d =4.5cm

(f) Flow without driftwood case

Fig. 24 Sediment discharge at downstream end and discharge reduction by grid dam due to driftwood jamming

driftwood jamming is also developed. To simulate the debris flow with driftwood capturing by grid or slit dam, a jamming model of driftwood and a deposition model behind a grid or slit dam are incorporated in a flow model of debris flow with driftwood. The parameters of the numerical simulation are as follows; Δx =5cm, Δy =1cm, Δt = 0.001sec, ρ = 1.0g/cm^3, ρ_m = 1.15g/cm^3, g = 980cm/sec^2, C_3= 0.48, n =0.04, C_* =0.65, C_{Dx} =1.0, C_{Dy} =1.0, δ_e =0.0018, δ_d =0.045, C_M =1.0 and K_{sd} =0.1.

Figs. 23 (a), (b), (c), (d) and (e) show the flow discharge at downstream end of the flume and reduction of outflow discharge by grid dam with debris flow capturing due to jamming of driftwood on a grid dam for the cases with driftwood D_d=3mm and L_d=3.5cm, D_d=3mm and L_d=4.0cm, D_d=3mm and L_d=4.5cm, D_d=4mm and L_d=3.5cm, and D_d=4mm and L_d=4.5cm, respectively. Debris flow is captured effectively by a grid dam due to the driftwood jamming. The simulated results of flow discharge passed through a grid dam and flow discharge without dam are quite close to the

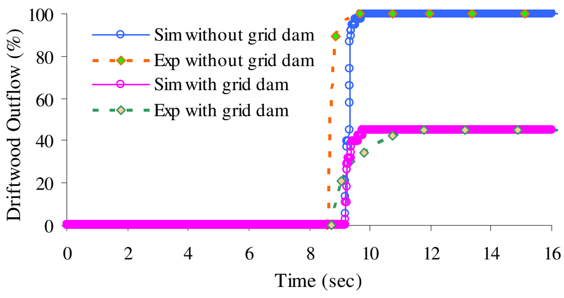

(a) With driftwood D_d=3mm and L_d =3.5cm

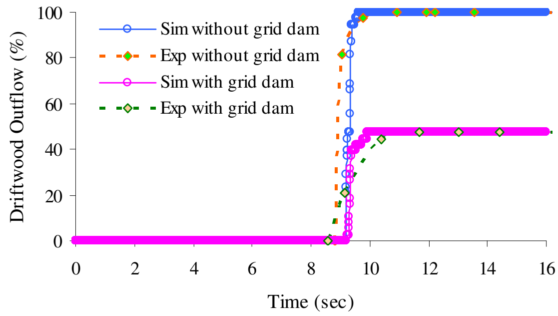

(b) With driftwood D_d=3mm and L_d =4.0cm

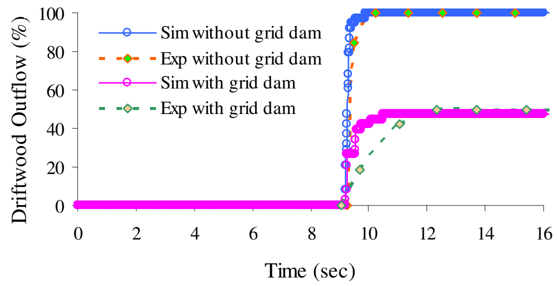

(c) With driftwood D_d=3mm and L_d =4.5cm

Fig. 25 Accumulated driftwood outflow at outlet of the flume, with grid dam, driftwood diameter D_d=3mm case

experimental results. Fig. 23 (f) shows the flow discharge without driftwood case, in which flow discharge is not reduced effectively by a grid dam with compared to the flow discharge with driftwood cases. From the results, outflow discharge is reduced by a grid dam more effectively in the cases with driftwood due to jamming of driftwood on a grid dam. The results of sediment discharge at downstream end of the flume with different sizes of driftwood cases are shown in Figs. 24 (a), (b), (c), (d) and (e). The sediment discharge is reduced by sediment deposition behind a grid dam due to

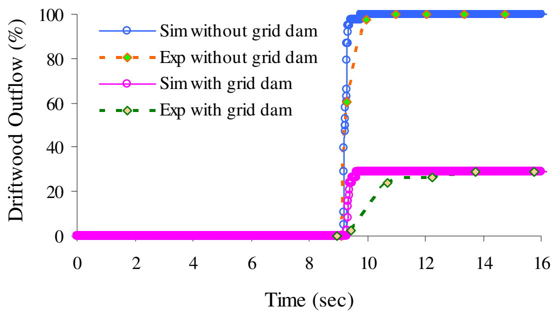

(a) With driftwood D_d=4mm and L_d =3.5cm

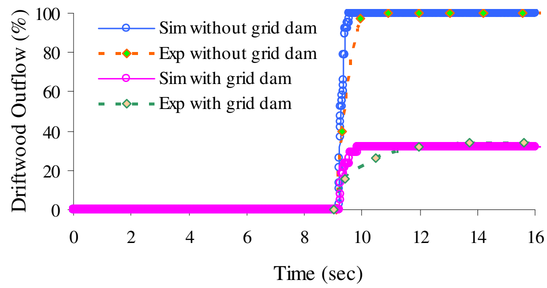

(b) With driftwood D_d=4mm and L_d =4.5cm

Fig. 26 Accumulated driftwood outflow at outlet of the flume, with grid dam, driftwood diameter D_d=4mm case

driftwood jamming on a grid dam. Fig. 24 (f) shows the sediment discharge at downstream end of the flume without driftwood case. The simulated results of outflow sediment discharge from a grid dam are also agreeable with the experimental results. The effect of driftwood jamming on sediment deposition behind a dam using developed deposition equation is well explained in the simulations. In the calculation, deposition due to blockage of grid dam by large boulders is also considered.

The results of percentage of temporal driftwood outflow at the downstream end of the flume in grid dam case with different sizes of driftwood are shown in Fig. 25 and Fig. 26 for driftwood diameter D_d=3mm and D_d=4mm cases, respectively. The percentage of driftwood outflow is the ratio of the number of pieces of driftwood outflow at downstream end to the total amount of driftwood supplied at the inflow boundary. The driftwood passed through a grid dam is reduced due to the driftwood jamming on grid dam. The number of pieces of the driftwood outflows from a grid dam

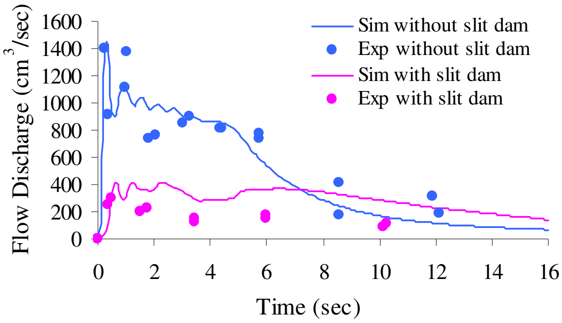

(a) Case with driftwood D_d=3mm and L_d =4.5cm

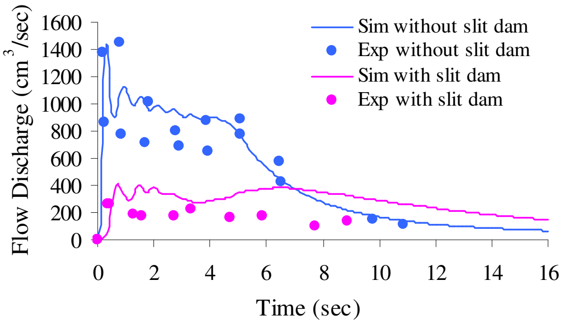

(b) Case with driftwood D_d=4mm and L_d =4.5cm

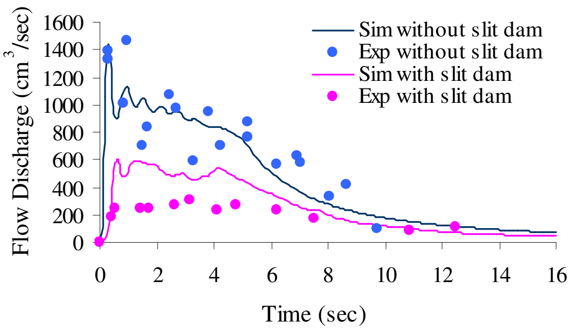

(c) Flow without driftwood case

Fig. 27 Flow discharge at downstream end of the flume with slit dam case

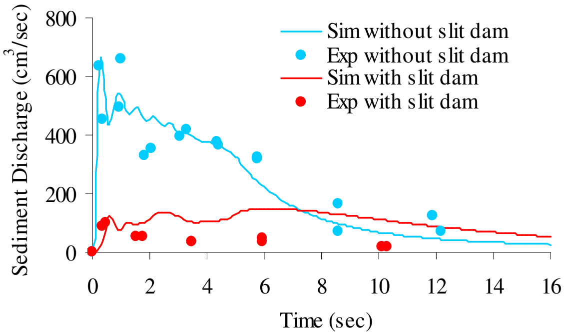

(a) Case with driftwood D_d=3mm and L_d =4.5cm

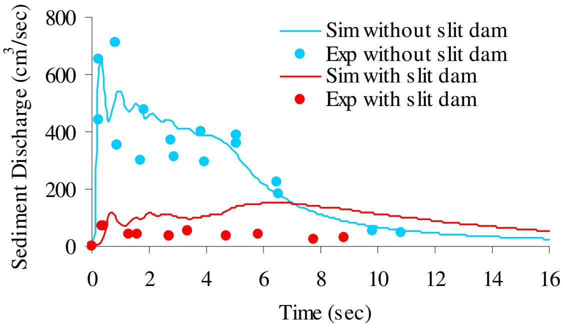

(b) Case with driftwood D_d=4mm and L_d =4.5cm

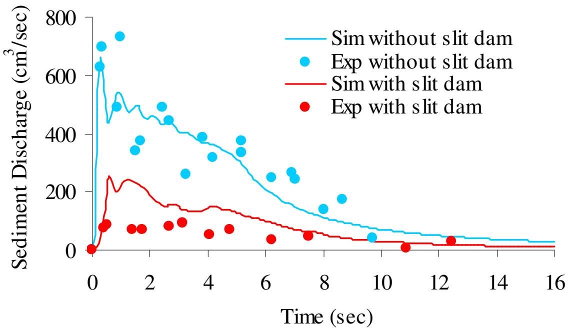

(c) Flow without driftwood case

Fig. 28 Sediment discharge at downstream end of the flume with slit dam case

based on the developed driftwood jamming model under the geometric conditions and probabilistic approaches are well explained in the numerical simulations. The simulated results of driftwood outflow time at the downstream end of the flume are also close to the results obtained from the experiments.

The results of flow discharge and reduction of flow discharge by slit dam at downstream end of the flume with and with out driftwood cases are shown in Fig. 27. Fig. 28 shows the results of sediment discharge at downstream end of the flume in the case of slit dam. The simulated results of flow discharge and sediment discharge passing through a slit dam are agreeable with the experimental results. The debris flow deposition behind a slit dam due to driftwood jamming is also well explained in the numerical simulations.

The results of percentage of temporal driftwood outflow at the downstream end of the flume in slit dam case with driftwood D_d=3mm and L_d=4.5cm and D_d=4mm and L_d=4.5cm are shown in Fig. 29.

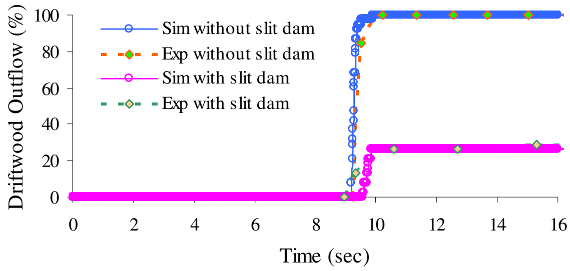

(a) With driftwood D_d=3mm and L_d =4.5cm

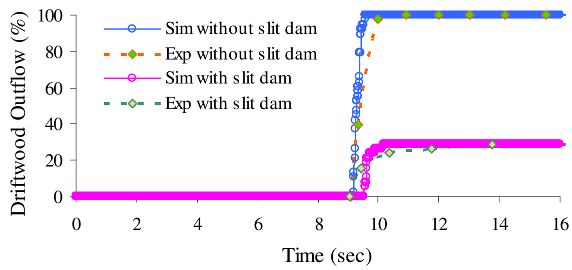

(b) With driftwood D_d=4mm and L_d =4.5cm

Fig. 29 Accumulated driftwood outflow at outlet of the flume with slit dam

The driftwood passed through a slit dam is reduced due to the driftwood jamming on slit dam. The jamming of driftwood on slit dam is well explained in the numerical simulations with compared to the experimental results.

7. Conclusions

A two-dimensional numerical model is developed for computing the characteristics of debris flow with driftwood. Numerical simulations and experimental works are carried out to determine the characteristics of debris flow with driftwood. Equations of the rotational motion and the translational motion of driftwood are evaluated dynamically in the Lagrangian form. A numerical model is developed with an interacting combination of Eulerian expression of the debris flow and Lagrangian expression of the driftwood, in which the fluctuation components of the position and the rotational angular velocity of the driftwood are dealt with stochastically. The position and rotational angular velocity of the driftwood fluctuate due to the collision of driftwood with boulders and disturbances on the flow surface during the collision of the sediment particles, which are considered in the diffusions coefficients. The scattering process of driftwood is described as a diffusion process and the diffusion coefficients are defined by the hydraulic experiments. The calculated results of frequency distribution of the longitudinal positions, the transverse positions and the rotational angular velocities of the driftwood are fairly good agreement with the experimental results.

The process of debris flow capturing by grid and slit dams due to jamming of driftwood is investigated. A numerical model is developed for computing the debris flow with driftwood capturing by open type check dams such as grid and slit dams. The jamming of driftwood on open type check dams is evaluated based on the geometric conditions and probabilistic approaches. A deposition velocity model is also developed to calculate the debris flow deposition due to driftwood jamming on a grid or slit dam. The flow and sediment discharge passing through a grid or slit dam are reduced due to driftwood jamming. The simulated results of flow discharge, sediment discharge and percentage of driftwood passed through a grid or slit dam are in good agreement with the experimental results.

References

Doi, Y., Minami, N., Yamada, T. and Amada, T. (2000): Experimental analysis of woody debris trapping by impermeable type sabo dam, filled with sediment -woody debris carried by debris flow-, Journal of the Japan Society of Erosion Control Engineering, Vol. 52, No. 6, pp.49-55 (in Japanese).

Egashira, S. (1993): Mechanism of sediment deposition from debris flow (part 1), Journal of the Japan Society of Erosion Control Engineering, Vol. 46, No. 1, ser.186, pp.45-49 (in Japanese).

Gotoh, H., Sakai, T. and Hayashi, M. (2002): Lagrangian model of drift-timbers induced flood by using moving particle semi-implicit model, Journal of Hydroscience and Hydraulic Engineering, JSCE, Vol. 20, No. 1, pp.95-102.

Honda, N. and Egashira, S. (1997): Prediction of debris flow characteristics in mountainous torrents, Proceedings of First Conference on Debris-Flow Hazards Mitigation: Mechanics, Prediction, and Assessment, California, ASCE, pp.707-716.

Huang, X. and Garcia, M. H. (1997): A perturbation solution for Bingham-plastic mudflows, Journal of Hydraulic Engineering, ASCE, Vol. 123, No. 11, pp.986-994.

Hunt, B. (1994): Newtonian fluid mechanics treatment of debris flows and avalanches, Journal of Hydraulic Engineering, ASCE, Vol. 120, No. 12, pp.1350-1363.

Inverson, R. M. (2003): The debris-flow rheology myth, Proceedings of the Third Conference on Debris-Flow Hazards Mitigation: Mechanics, Prediction, and Assessment, Switzerland, Rotterdam, pp.303-314.

Katatani, M. and Yamada, T. (2006): Study on new type slit sabo dam development for reduction of slit blockade by drift woods, Journal of the Japan Society of Erosion Control Engineering, Vol. 59, No. 36, pp.23-31 (in Japanese).

Nakagawa, H., Inoue, K., Ikeguchi, M. and Tsubono, T. (1995): Behavior of driftwood and the process of its damming up, Journal of Hydroscience and Hydraulic Engineering, JSCE, Vol. 13, No. 2, pp.55-67.

Nakagawa, H., Takahashi, T. and Ikeguchi, M. (1994): Driftwood behavior by overland flood flows, Journal of Hydroscience and Hydraulic Engineering, JSCE, Vol. 12, No. 2, pp.31-39.

Nakagawa, H., Takahashi, T. and Satofuka, Y. (2000): A debris-flow disaster on the fan of the Harihara River, Japan, Proceedings of the Second International Conference on Debris-Flow Hazards Mitigation: Mechanics, Prediction, and Assessment, Taiwan, Balkema, Rotterdam, pp.193-201.

Nakagawa, H., Takahashi, T., Sawada, T. and Satofuka, Y. (1996): Design hydrograph and evacuation planning for debris flow, Annuals of the Disaster Prevention Research Institute, Kyoto University, No. 39 B-2, pp.347-371 (in Japanese).

Ozaki, Y., Kamogawa, Y., Mizuyama, T., Kasai, S. and Shima, J. (1998): A debris flow with woody debris trapped by a steel-pipe gridded sabo dam, Journal of the Japan Society of Erosion Control Engineering, Vol. 51, No. 2, pp.39-44 (in Japanese).

Sabo Department, Ministry of Construction, Japan (2000): Guideline for driftwood countermeasures, Guideline of Ministry of Construction, Japan.

Satofuka, Y. and Mizuyama, T. (2006): Numerical simulation on debris flow control by a grid dam, The 6th Japan-Taiwan Joint Seminar on Natural Hazard Mitigation (in CD-ROM).

Shimizu, Y. and Osada, K. (2008): Numerical simulation on the driftwood behavior in open-channel flows by using distinct element method, The Eighth International Conference on Hydro-Science and Engineering, Nagoya, Japan.

Shrestha, B. B., Nakagawa, H., Kawaike, K. and Baba, Y. (2008): Numerical simulation on debris-flow deposition and erosion processes upstream of a check dam with experimental verification, Annuals of the Disaster Prevention Research Institute, Kyoto University, No. 51 B, pp.613-624.

Shrestha, B. B., Nakagawa, H., Kawaike, K., Baba, Y. and Zhang, H. (2009): Numerical simulation on debris-flow with driftwood and its capturing due to jamming of driftwood on a grid dam, Annual Journal of Hydraulic Engineering, JSCE, Vol. 53, pp.169-174.

Takahashi, T. (1991): Debris flow, Monograph Series of IAHR, Balkema.

Takahashi, T. (2007): Debris flow: Mechanics, Prediction and Countermeasures, Proceedings and Monographs, Taylor & Francis/Balkema.

Takahashi, T., Nakagawa, H., Harada, T. and Yamashiki, Y. (1992): Routing debris flows with particle segregation, Journal of Hydraulic Engineering, ASCE, Vol. 118, No. 11, pp.1490-1507.

Takahashi, T., Nakagawa, H., Satofuka, Y. and Wang, H. (2001): Stochastic model of blocking for a grid-type dam by large boulders in a debris flow, Annual Journal of Hydraulic Engineering, JSCE, Vol. 45, pp.703-708 (in Japanese).

透過型砂防ダムによる流木を伴う土石流の捕捉過程

Badri Bhakta SHRESTHA*・中川一・川池健司・馬場康之・張浩

*京都大学大学院工学研究科

要　旨

流木を含む土石流の特性及び, グリッドダム・スリットダムに代表される透過型砂防ダムによるこれの捕捉過程をシミュレートする二次元数値解析モデルを構築した。数値解析モデルは, 土石流のオイラー的挙動解析法と流木のラグランジュ的運動追跡法の組み合わせにより構成しており, 流木が存在する座標の変動成分及び流木の回転角速度については確率的にこれを与えた。透過型砂防ダムによる流木の阻害については, 流木の幾何学的状態及び確率的手法により評価を行った。数値解析により, 実験結果と適合する流出量・堆積量・下流端での流木通過率を得た。

キーワード: 土石流, 流木, 透過型砂防ダム, 捕捉過程, 数値解析